Liquid Cooled Battery Thermal Management System for 3S2P Li-Ion Battery Configuration

Divya D. Shetty, Aditya Nair, Rishab Agarwal, and Kshitij Gupta

Abstract Lithium-ion batteries are the future of the automotive industry. Due to their zero-emission technology, lithium-ion powered electric vehicles are hyped as the power source of the future. However, one of the main drawbacks of the cell is its high heat generation, which, in turn, affects the performance of the vehicle. Currently, research is being conducted into developing an efficient battery thermal management system (BTMS). The present study will be looking into developing a liquid battery thermal management system. To determine the efficiency of the cooling system, heat generation on a smaller battery pack was modelled with the help of the MSMD model on Ansys fluent. A smaller battery pack of a 3s2p configuration was selected to validate the results. The parameters of the cell were available on the datasheet. Materials were selected based on the data present on Ansys fluent. The simulation was conducted for two discharge rates 1C and 2C. As a result, it was observed that for the 3s2p configuration, the maximum temperatures go up to 320 K and 335 K for a discharge rate of 1C and 2C, respectively. After this, the battery pack is subjected to a liquid thermal management system. The effect of various mass flow rate on temperature are as follows at flow rate of 1e-5 the maximum temperature decreases by 5.31%, whereas the maximum temperatures at 1e-4 and 1e-3 flowrate decreases by 5.93% and 6.01% respectively at 1C discharge rate. In case of 2C discharge rate, at the mass flow rate of 1e-5, the maximum temperature decrease is by 8.65%, whereas for 1e-4 and 1e-3, the maximum temperature decrease is by 9.85% and 10.14%, respectively. A crossflow design is adopted and was compared with the normal flow; it is observed that there is no significant effect of flow direction on temperature.

Keywords Li-ion battery · Maximum temperature · Discharge rate

D. D. Shetty (✉) · A. Nair · R. Agarwal · K. Gupta
Department of Aeronautical and Automobile Engineering, Manipal Institute of Technology, Manipal Academy of Higher Education, Manipal, Karnataka 576104, India
e-mail: Shetty.divya@manipal.edu

V. Krishna et al. (eds.), *Recent Advances in Hybrid and Electric Automotive Technologies*, Lecture Notes in Mechanical Engineering,
https://doi.org/10.1007/978-981-19-2091-2_18

1 Introduction

Electric vehicles are the future of the automotive industry. With the rising prices of crude oil and the depleting natural resources around the world, we are forced to look for alternative ways of providing energy to the vehicle. The experts in the automobile industry thus came up with a solution to this problem by attaching and trying to power the car with a battery, motor and generator, thus giving rise to Electric Vehicles, commonly known as EVs [1]. These EVs are powered by a battery connected to a motor, which, in turn, drives the wheels. These motors act as a generator also, thus recharging the battery as the vehicle moves. Electric Vehicles are being used in passenger vehicles and motorsports with the introduction of Formula-E [2]. A Lithium-ion battery is the most popular battery used in Electric vehicles. There exist several cells with similar chemistry to that of Li-ion cells like Li-nickel-manganese-cobalt (NMC), Li-phosphate and Li manganese, with each cell being advantageous over its peers in a few sectors [3]. However, holistically, Li-ion cells have been found to be superior, chemistry-wise, to drive the powertrain of an electric vehicle for the following reasons: Higher energy density, high power density and longer cycle life [4]. In addition to high energy and power density, lithium-ion batteries have shown high life cycle, particularly when operated under shallow cycling conditions [3].

One of the major challenges is keeping the battery pack cool even after long durations of discharging and charging cycles. The solution to this problem is still in the early stages of research and development and still requires a lot of attention. This heating issue in the battery pack occurs due to the following reasons [6]: a. Thermal Runaway [7], b. Ageing, c. Gassing and d. Cost of production. In many cases, Panasonic, the supplier of cells to tesla, makes use of a Lithium cobalt aluminium configuration [8]. The need for a battery management system has increased over the years because the companies are also incorporating more and more motors in their vehicles, for example, Rimac, an electric supercar maker who has successfully developed an electric hypercar by the name of Rimac concept 1, which drives on four motors, each for one wheel. Due to this the battery heat up exponentially, thus becoming less effective in the upper region of the torque curve [7]. Another reason for a battery management system includes increasing the efficiency of the battery and the vehicle, thus increasing the range of the vehicle. Under normal use, an electric vehicle's batteries like to be in the 15 to 35 °C range [6].

1.1 Types of Battery Cooling Systems

The different types of battery thermal management systems are air-cooled, liquid-cooled, PCM- based, thermoelectric and heat pipes. The air cooled is further classified as active and passive, for active air-cooling system, some external means are required to circulate air through cooling channels. In a passive system, the atmospheric air will directly come in contact with the cell surface [9]. Aside from air, the liquid is

another heat transfer fluid that can be used to transmit heat. For thermal management systems, there are two types of liquids. Mineral oil, for example, is a direct contact liquid that can come into direct touch with the battery cells. The other is an indirect contact liquid, such as a combination of ethylene glycol and water, that can only make indirect contact with the battery cells [10]. In a direct contact system, the battery pack is directly submerged in liquid, and in an indirect contact liquid-cooled system, the fluid is circulated through a cooling jacket by some external means [11]. Heat is absorbed by PCM during melting and stored as latent heat until it reaches its maximum. The temperature is held at a melting point for a length of time, and the increase in temperature is postponed. As a result, PCM is employed in battery temperature management systems as a conductor and buffer. To manage the battery temperature, a PCM is always paired with an air-cooling system or a liquid-cooling system [7].

1.2 Innovations in Battery Solutions

Cylindrical lithium-ion batteries are preferred over their counterparts due to their high power density and ability to be produced faster. Hence, the following report summarized various literature of cooling systems for cylindrical batteries [10]. Zhao et al. [10] conducted research around a novel cooling system. The construction of the cooling system is as follows: the battery is enclosed in a cylindrical shell that consists of channels, through which liquid flows, called the liquid cooling cylinder (LCC). A liquid cooling plate (LCP) supplies the cooling liquid to the LCC and acts as a reservoir at the outlet of the LCC. The author investigated four parameters—no of channels, inlet size, mass flow rate and flow direction. The trend observed is that maximum temperature keeps decreasing with an increasing number of channels when the number of channels is greater than 4 up to 8 channels. In the case of maximum temperature difference ΔT, there is a decreasing trend found with increasing channels, but the effect of cooling decreases. In case of inlet size, it can be concluded that the capacity of heat exchange is enhanced first and then weaken along with the rising of entrance size. Flow direction also plays an important role. When the inlet and outlet were located on the same side, there was a change and a decrease in the maximum temperature. However, due to the challenges in designing a circulatory system around this, this method was not advised to be implemented.

Wang et al. [12] modified the above system by designing a transfer contact surface (TCS), which is a diamond curved shape in contact with 3 cells at a time. While investigating mass flow rate, the heat generation process was divided into three time periods: 0–100 s, 100–600 s and 600–720 s. During phase 1, the max temperature and temperature difference rise irrespective of the mass flow rate. In the second phase, the temperature can be kept constant at 1×10–4 kg/s. There is not a significant effect of cooling on the decrease of maximum temperature difference. Upon investigating inner diameter, it was found that decreasing inner diameter increases the velocity, which would lead to the assumption of increased heat transfer coefficient. However,

decreasing the diameter decreases the contact surface. Hence, overall, there is little effect of diameter on cooling performance. The Temperature increases gently by decreasing the height of the inlet. The optimum height is obtained when h = 55 mm. By increasing the contact angle, the max temperature and temperature difference reduce as the contact area increases.

Jiang et al. [13] investigated the tesla cooling system. However, a critical analysis was conducted, and a comparison was made between two different approaches adopted. In the multiple short channel approach, the U-bend is removed, and two short channels are compared with the long channel. It is observed that the short channels yield a lesser maximum temperature than the u-bend channel. This can be due to the less flow resistance caused due to the U-bend. The magnification of the contact area was also investigated. It was found that there is a decrease in the maximum temperature yield. A greater outcome of the system is the temperature uniformity of the cell obtained. Mahmud et al. [14] implemented the idea of thermoelectric cooling to cool a battery. The thermoelectric module used is connected electrically in series and thermally in parallel. There are aluminum sinks with a cooling fan and channels containing coolant to cool the hot side of the TEC module. Hence, it is a conjunction of Air and liquid cooling. The maximum temperature was investigated, and the test was first conducted without the TEC module, in the presence of water alone and then in the presence of air alone, and then with the TEC module. In comparison, the TEC module showed a drastic reduction in temperature. The cooling rate was found to be double when compared to the water and air only conditions.

Yang et al. [15] implemented a composite PCM (Composite PCM) to cool the battery pack. The C-PCM is made by first melting paraffin, and then it is melted together with expanded graphite. This is done to increase the thermal conductivity of the PCM. Low-density polyethylene is introduced. Upon discharge of the battery pack, it was found that the L-CPCM performs better cooling performance. However, during higher discharge rates above 3C, the temperature of the battery was beyond the safe limit of the lithium-ion battery. To tackle this issue, an aluminium fin was used as a heat sink to dissipate heat further away from the system. Upon experimentation, it was found that the aluminium fin has a positive effect on the cooling performance of the battery. At higher discharge rates, the maximum temperature has been found to be well within the safe limits of the lithium-ion battery. Yulong Dinga et al. [16] investigated the use of metallic foam in conjunction with a PCM, and a copper pipe module containing a coolant. In this paper. A comparison is made between paraffin wax alone in the material module and copper foam/paraffin wax (C-PCM) as a material module. After discharge operation at 1800s, the outlet temperature of the copper pipe is more in case of the C-PCM, than in the standalone paraffin setup. The outlet temperature is also found to increase with increasing velocity. In case of the battery surface, the temperature of just PCM was found to rise by 16 degrees to 39 °C. However, in case of C-PCM, the temperature of the battery surface was found to be 25 °C. This is because the metallic copper foam offers greater thermal conductivity, which is less in case of paraffin wax.

From the literature, it is observed that the advantages of liquid cooling systems are as follows: (a) A liquid cooling system helps in effectively controlling the maximum

temperature and temperature difference of the cell. (b) Making use of nanofluids can help control the temperature at a velocity lesser than that used for a normal coolant, hence preventing excessive power consumption. (c) A liquid system can also be used to heat the battery pack in cold countries where ambient temperatures are below the freezing point. Disadvantages of a liquid cooling system are as follows: (a) Due to unforeseen circumstances, accidental leakage of the coolant may occur, leading to damage to the battery pack. (b) A liquid cooling system is heavier compared to other cooling systems. Hence, in order to reduce weight, a microchannel may be used. (c) A liquid cooling system consumes additional power to circulate the coolant across the battery pack. Usage of microchannels in order to reduce weight may increase the pressure drop due to which the power consumption will increase. Despite the disadvantages, the advantages outweigh them, and hence is a system preferred by many automotive companies to implement on a large scale.

2 Methodology

2.1 Modelling and Meshing

3s2p

In the present analysis, a battery pack consisting of six cells is considered. The cell used in the 3s2p configuration as shown in Fig. 1 is 18650 Li-ion cells, the diameter of the cell is 18 mm and length of the cell is 650 mm. The configuration of the battery pack is 3 in series and 2 in parallel. After naming each part of the cell, a battery connection is established by Ansys fluent. The batteries had a centre-to-centre distance of 3 mm across all directions. The cells were placed in an aluminium block. Due to its higher heat transfer coefficient, heat generated by the battery would be rapidly transferred, hence aluminium was selected as the material. Twelve channels were cut out from the aluminium block as represented in Fig. 2, which act as a channel for the coolant to flow through. The geometrical parameters of aluminium block are as follows (Fig. 3): length, breadth and height of the block are 86 mm, 64 mm and 65 mm, respectively. The diameter of the channel pierced through the aluminium block is 8 mm. Figure 1 is the 3D model of Li-ion cell with a 3s2p configuration.

Meshing

The fluid channel and body are meshed using the quad and tri elements. The cell body and cell terminals were meshed using the sweep method and the rest of the body was meshed with tetrahedral cells. The mesh element size is given as 8.49e–003 m,4 inflation layer was used near fluid channels in aluminium block to better simulate the effect of the boundary layer. The battery connections are setup using the dual potential Multi Scale Multi Domain (MSMD) model in Ansys. This model solves the potential across two domains: positive and negative zones of the cell. The cell

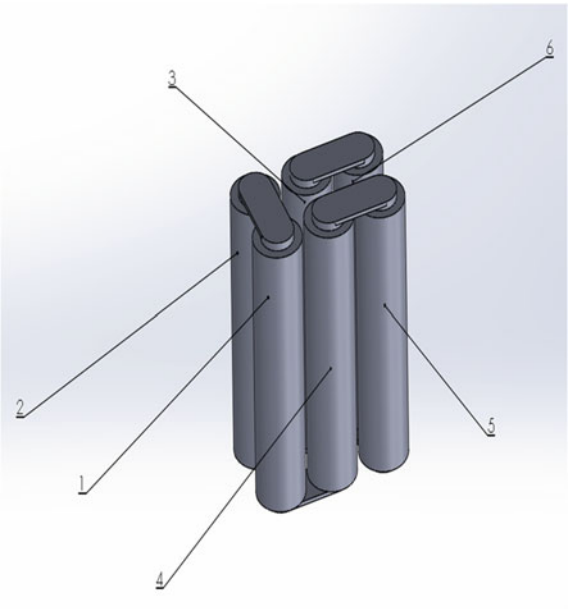

Fig. 1 Cell arrangement

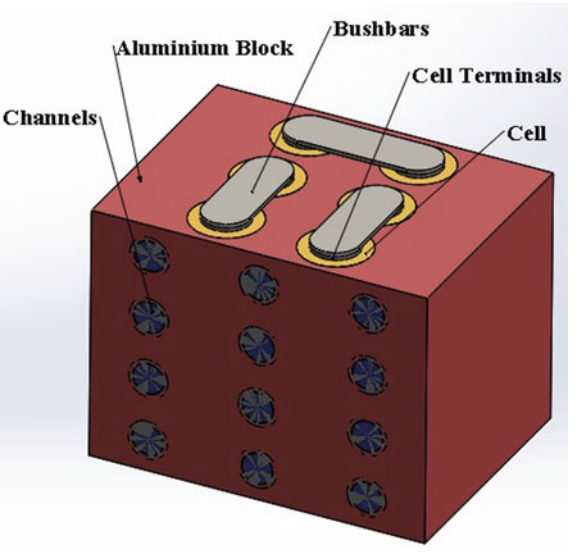

Fig. 2 Entire thermal management system

capacity of a single cell is as follows: Nominal Cell Capacity—3.5 Ah, Min Stop Voltage—2.6 V and Max Stop Voltage—4.2 V.

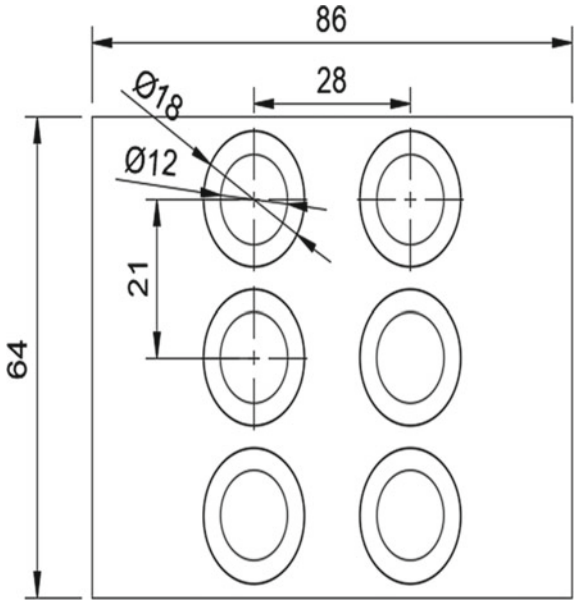

Fig. 3 Dimensions of thermal management system

2.2 Boundary Conditions

In the given setup, there are 12 inlets and outlets. The inlet values are mass-flow-rate for inlet condition. The inside of the channels was assigned a no-slip condition. The inlet temperature of the fluid is assumed to be at room temperature, i.e., 300 K. The battery pack parameters, as well as materials used for cell, are discussed in Table 1 and Table 2, respectively. The walls of the cell, terminals, and busbars were allotted to the material based on the data given in the Ansys fluent user guide (Table 3). The UDS diffusivity for busbars and terminals is a user-defined function in Ansys. The UDS diffusivity for the cell is UDS-0 = 1.19e06, UDS-1 = 9.83e05 [17].

2.3 Thermal Behaviour

In this case, LG 18650 cell was investigated. To obtain the thermal behaviour, the dual potential multi-scale multi-domain model is provided within Ansys fluent. In this method, governing equations are solved across two domains to simulate the current drawn, and hence heat generated by the battery is based on various discharge rates. To determine the various coefficients, a voltage versus time graph is obtained for the cells by inserting input using the TUI console. Temperature corrections are obtained using the following equations [17].

Table 1 Battery pack parameters [17]

MSMD parameters		
Parameter	Value	Unit
Cell parameters		
Nominal cell capacity	3.5	mAh
C-rate	1	
Min. stop voltage	2.6	V
Max stop voltage	4.2	V
NTGK polarization parameters		
Initial DOD	0	
Reference capacity	7	mAh
U coefficient: a1, a2, a3, a4, a5	4.19, −1.711, 8.90, −37.28, 62.418, −35.26	
Y coefficient: b1, b2, b3, b4, b5	66.196, −397.891, 2706.86, −7378.21, 8258.162, −3235.86	
Temperature corrections: C1, C2	0,0	

Table 2 Cell material [17]

Density	678	J/kg K
Specific Heat	18.4	W/m–K
Thermal Conductivity	1.19×10^6	kg/m-s
UDS-0	9.83×10^5	kg/m-s
UDS-1	3.541×10^7	Siemens/m
Electrical Conductivity	678	J/kg K

Table 3 Terminal material [17]

Density	8978	kg/m^3
Specific Heat	381	J/kg K
Thermal Conductivity	387.6	W/m–K
UDS diffusivity	Model Defined	kg/m-s
Electrical Conductivity	1×10^7	Siemens/m

$$\frac{\delta_p C_p T}{\delta T} - \nabla \cdot (k \nabla T) = q \tag{1}$$

$$\nabla \cdot (\sigma_+ \nabla \sigma_+) = -j \tag{2}$$

$$\nabla \cdot (\sigma_- \nabla \sigma_-) = j \tag{3}$$

Here, $\varnothing$ is electric potential, σiselectricconductivity, and neg and pos refer to negative and positive electrode

$$U = \left[\sum_{n=0}^{3} b_n (DOD)^n\right] - C_2\left(T - T_{ref}\right) \tag{4}$$

$$Y = \left[\sum_{n=0}^{5} b_n (DOD)^n\right] exp\left[-C_1\left(\frac{1}{T} - \frac{1}{T_{ref}}\right)\right] \tag{5}$$

$$U = a_0 + a_1 DOD + a_2 DOD^2 + a_3 DOD^3 + a_4 DOD^4 + a_5 DOD^5 \tag{6}$$

$$Y = b_0 + b_1 DOD + b_2 DOD^2 + b_3 DOD^3 + b_4 DOD^4 + b_5 DOD^5 \tag{7}$$

Here, DOD means the depth of discharge of the cell.

C-rate is the discharge rate at which the battery discharges relative to the maximum battery capacity of the cell. C-rate is calculated using the following formula [19]:

$$C = \frac{\text{Current drawn(A)}}{\text{Capacity(Ah)}} \tag{8}$$

3 Result Analysis

3.1 Thermal Behaviour

3series2parallel configuration

After simulating the given battery pack at 1C and 2C discharge rates, an analysis of the maximum temperature of each cell in the pack was carried out as shown in Figs. 3 and 4.

After simulating the given battery pack at 1C and 2C discharge rates, the maximum temperature difference of each cell in the pack was analyzed as shown in Figs. 3 and 4. From Fig. 5, it is observed that Cell 3 has attained the highest temperature, whereas cell 1 has attained the lowest temperature. It was also observed that the temperature change for all the cells is greater than 15 K for 1C and 28 K for 2C, posing a threat of instability to the battery pack. It is noticed that the battery pack gets heated the most at the centre. Hence, while designing the thermal management system, it was important to make sure the centre of the battery pack is cooled effectively. To summarize the thermal distribution results:(a) The heat is generated due to joule heat and electrochemical heat source. (b) From Fig. 5a, c, it can be concluded that the maximum temperatures go up to 320 K and 335 K for discharge rates of 1C and 2C, respectively, for configuration of 3s2p. (c) It was also interesting to note that the temperatures across the parallel connections were the highest. These temperatures were well beyond the tolerable limit of the lithium-ion battery. Hence, to prevent

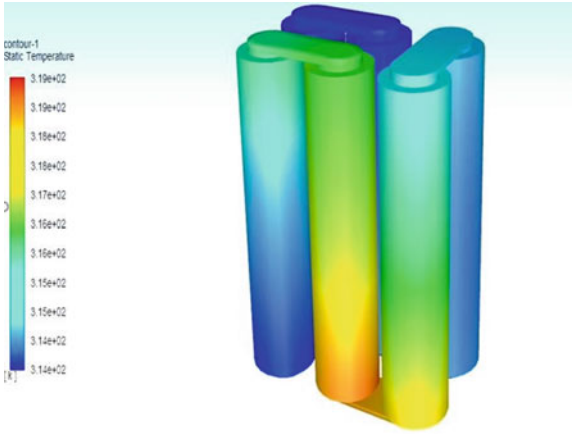

Fig. 4 Temperature distribution for 1C

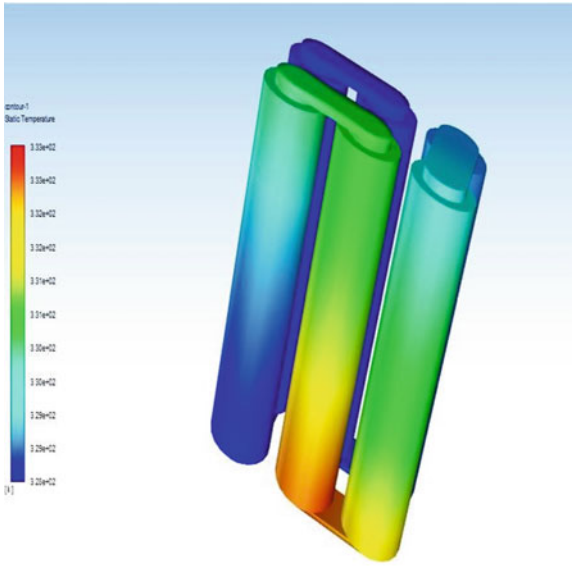

Fig. 5 Temperature distribution for 2C

thermal runaway of the battery, it is important to maintain these temperatures within the optimum operating range of a lithium-ion cell.

3.2 Cooling of 3s2p

Effect of Mass flow rate: In this section, the effect of mass flow rate was investigated. Figure 6 below depict the maximum temperature and temperature difference of the

battery pack with cooling at a discharge rate of 1C and 2C. For the first two minutes of runtime at a discharge rate of 1C, the rise in temperature is the same irrespective of the mass flow rate. This is because the temperature difference between the cell and the fluid is far lesser than the heat generation of the battery. Beyond this, the cooling effect of the mass flow rate influences the temperature of the cell as shown in Fig. 6. For the mass flow rate of 1e-5 as shown in Fig. 6a, the maximum temperature at the end of the simulation is close to 303 K (5.31% decrease), whereas the maximum temperatures at the end of the simulation time for 1e-4 and 1e-3 are 301 K (5.93% decrease) and 300.75 K (6.01% decrease), respectively, for 1C discharge rate. In case of a discharge rate of 2C (Fig. 6c), the mass flow rate of 1e-5 results in a maximum temperature of 306 K (8.65% decrease), whereas for 1e-4 and 1e-3, the maximum temperatures were 302 K (9.85% decrease) and 301 K (10.14% decrease). The temperature difference is defined as the difference between the maximum and minimum temperature of the cell. It is important to maintain a temperature difference as low as possible to prevent thermal runaway issues in the cell. With respect to 1C, for all mass flow rates, the temperature difference lies within 1 K as represented in Fig. 6b. For a discharge rate of 2C, the mass flow rate of 1e-3 is the most effective, keeping it within 1 K as depicted in Fig. 6d.

Effect of direction of flow

In the following case, the direction of flow for the middle channels has been reversed and its effect has been investigated and compared with the normal flow as depicted in Fig. 7. For this case, a mass flow rate of 1e-4 was chosen and discharge rates of 1C and 2C were applied. After the simulation, it is noticed that there is not any

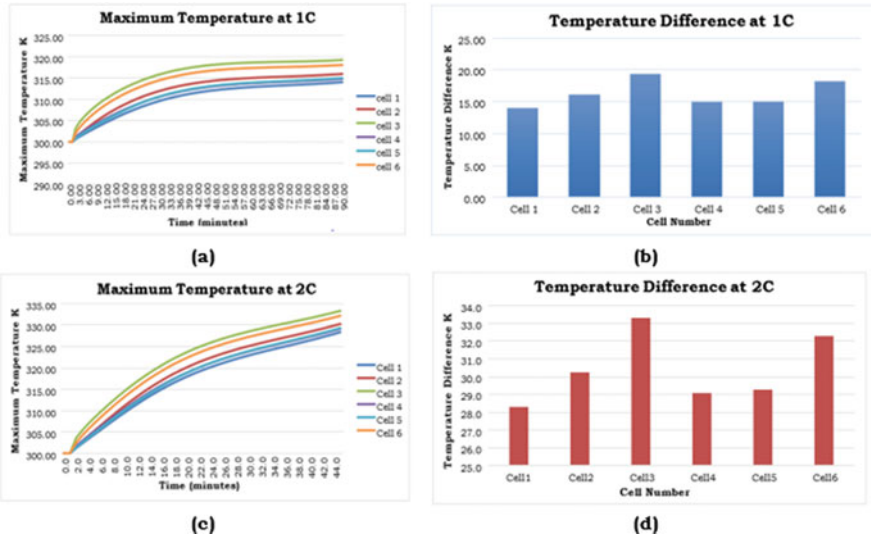

Fig. 6 Maximum temperature at (**a**) 1C Rate (**c**) 2C rate and temperature difference of the individual cell at (**b**) 1C (**d**) 2C without a thermal management system

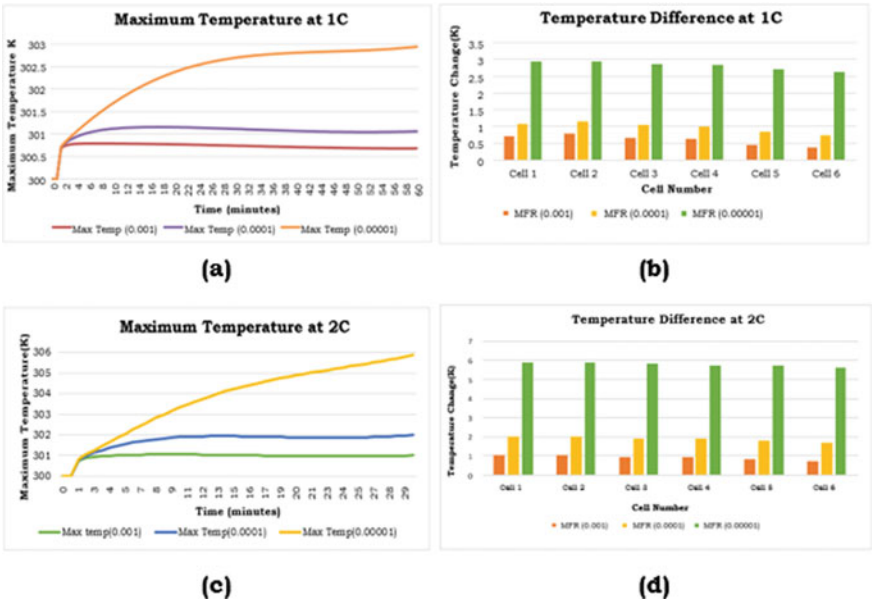

Fig. 7 Maximum temperature at (**a**) 1C Rate (**c**) 2C Rate and Temperature difference of the individual cell at (**b**) 1C (**d**) 2C with thermal management system at different mass flow rates

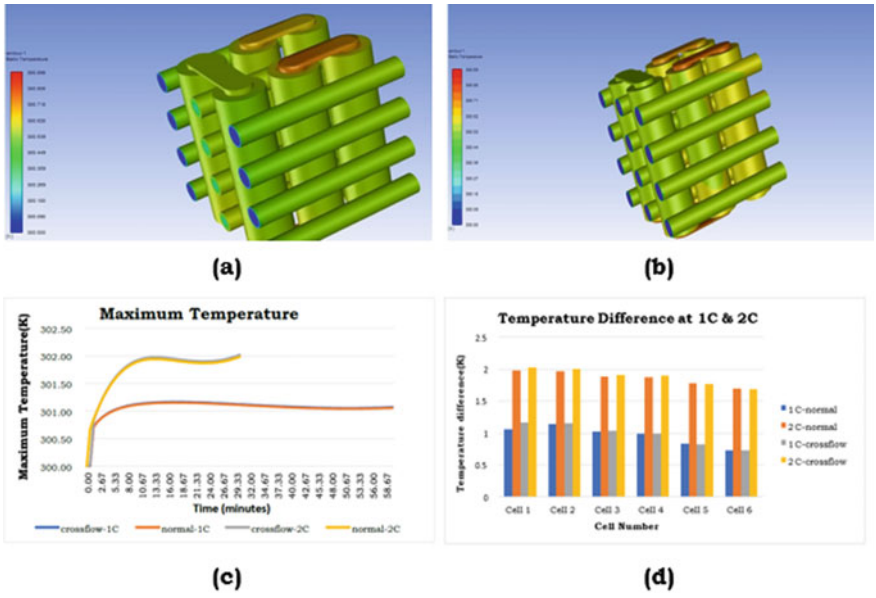

Fig. 8 Temperature distribution at (**a**) 1C Rate (**b**) 2C Rate and comparison of maximum temperature rise as well as Temperature difference at normal flow and crossflow (**b**) 1C (**d**) 2C

significant effect of the flow direction on the temperature and temperature difference of the battery pack as represented in Fig. 7.

4 Conclusion

Due to thermal issues surrounding lithium-ion batteries, the efficiency of the battery pack is reduced and the cost of the battery pack is increased. Hence, to solve these issues, a cooling system is the need of the hour. A lithium-ion cell best operates in the range of 20–35 °C. Hence, the objective of the liquid thermal management system is to maintain the temperature of these cells in a safe operating range. First, the discharge rates were chosen, in this case, 1C and 2C, and the temperatures were recorded. (a) From the results obtained, it can be concluded that the maximum temperatures go up to 320 K and 335 K for discharge rates of 1C and 2C, respectively, for configuration of 3s2p. (b) After this, the battery pack is subjected to a liquid thermal management system of various mass flow rates and recorded. For the mass flow rate of 1e-5, the maximum temperature at the end of the simulation is close to 303 K (5.31% decrease), whereas the maximum temperatures at the end of the simulation time for 1e-4 and 1e-3 are 301 K (5.93% decrease) and 300.75 K (6.01% decrease), respectively, for 1C discharge rate. In case of a discharge rate of 2C, the mass flow rate of 1e-5 results in a maximum temperature of 306 K (8.65% decrease), whereas for 1e-4 and 1e-3, the maximum temperatures were 302 K (9.85% decrease) and 301 K (10.14% decrease). (c) A crossflow design is adopted and was compared with the normal flow. It is observed that there is no significant effect of flow direction on temperature.

References

1. Khurana A, Kumar VVR, Sidhpuria M (2020) A Study on the Adoption of Electric Vehicles in India: The Mediating Role of Attitude. Vision 24(1):23–34. https://doi.org/10.1177/0972262919875548
2. Gelmanova ZS et al (2018) Electric cars. Advantages and disadvantages. J Phys Conf Ser 1015(5). https://doi.org/10.1088/1742-6596/1015/5/052029.
3. Iclodean C, Varga B, Burnete N, Cimerdean D, Jurchiş B (2017) Comparison of different battery types for electric vehicles. In: IOP Conf. Ser. Mater. Sci. Eng., vol 252, no 1. https://doi.org/10.1088/1757-899X/252/1/012058.
4. Scrosati B, Garche J (2010) Lithium batteries: Status, prospects and future. J Power Sources 195(9):2419–2430. https://doi.org/10.1016/j.jpowsour.2009.11.048
5. Miles MH (2008) Lithium batteries using molten nitrate electrolytes, 3:39–42. https://doi.org/10.1109/bcaa.1999.795958
6. Smith J, Singh R, Hinterberger M, Mochizuki M (2018) Battery thermal management system for electric vehicle using heat pipes. Int J Therm Sci 134(June 2017):517–529. https://doi.org/10.1016/j.ijthermalsci.2018.08.022
7. Katoch SS, Eswaramoorthy M (2020) A detailed review on electric vehicles battery thermal management system. In: IOP Conf. Ser. Mater. Sci. Eng., vol 912(4). https://doi.org/10.1088/1757899X/912/4/042005

8. Nitta N, Wu F, Lee JT, Yushin G (2015) Li-ion battery materials: present and future. Mater Today 18(5):252–264. https://doi.org/10.1016/j.mattod.2014.10.040
9. Li J, Zhu Z, Zhu Z (2014) Battery thermal management systems of electric vehicles, 79
10. Zhao J, Rao Z, Li Y (2015) Thermal performance of mini-channel liquid cooled cylinder-based battery thermal management for cylindrical lithium-ion power battery. Energy Convers Manag 103:157–165. https://doi.org/10.1016/j.enconman.2015.06.056
11. Deng Y et al (2018) Effects of different coolants and cooling strategies on the cooling performance of the power lithium ion battery system: a review. Appl Therm Eng 142(April):10–29. https://doi.org/10.1016/j.applthermaleng.2018.06.043
12. Lai Y, Wu W, Chen K, Wang S, Xin C (2019) A compact and lightweight liquid-cooled thermal management solution for cylindrical lithium-ion power battery pack. Int J Heat Mass Transf 144:118581. https://doi.org/10.1016/j.ijheatmasstransfer.2019.118581
13. Zhao C, Sousa ACM, Jiang F (2019) Minimization of thermal non-uniformity in lithium-ion battery pack cooled by channeled liquid flow. Int J Heat Mass Transf 129:660–670. https://doi.org/10.1016/j.ijheatmasstransfer.2018.10.017
14. Lyu Y, Siddique ARM, Majid SH, Biglarbegian M, Gadsden SA, Mahmud S (2019) Electric vehicle battery thermal management system with thermoelectric cooling. Energy Rep 5:822–827. https://doi.org/10.1016/j.egyr.2019.06.016
15. Lv Y, Yang X, Li X, Zhang G, Wang Z, Yang C (2016) Experimental study on a novel battery thermal management technology based on low density polyethylene-enhanced composite phase change materials coupled with low fins. Appl Energy 178:376–382. https://doi.org/10.1016/j.apenergy.2016.06.058
16. Zhao Y, Zou B, Li C, Ding Y (2019) Active cooling-based battery thermal management using composite phase change materials. Energy Procedia 158:4933–4940. https://doi.org/10.1016/j.egypro.2019.01.697
17. Gümüşsu E, Ekici Ö, Köksal M (2017) 3-D CFD modeling and experimental testing of thermal behavior of a Li-Ion battery. Appl Therm Eng 120:484–495. https://doi.org/10.1016/j.applthermaleng.2017.04.017
18. Ravnik J, Kerget L, Hriberek M (2010) Analysis of three-dimensional natural convection of nanofluids by BEM. Eng Anal Bound Elem 34(12):1018–1030. https://doi.org/10.1016/j.enganabound.2010.06.019
19. Zhang H, Li C, Zhang R, Lin Y, Fang H (2020) Thermal analysis of a 6s4p Lithium-ion battery pack cooled by cold plates based on a multi-domain modeling framework. Appl Therm Eng 173(December 2019):115216. https://doi.org/10.1016/j.applthermaleng.2020.115216